arXiv:1204.5940v3 [physics.atom-ph] 2 May 2012

Opto-mechanical measurement of micro-trap via nonlinear cavity enhanced Raman scattering spectrum

Lin Zhang
College of physics and Information Technology, Shaanxi Normal University, Xi'an 710061, China

High-gain resonant nonlinear Raman scattering on trapped cold atoms within a high-fineness ring optical cavity is simply explained under a nonlinear opto-mechanical mechanism, and a proposal using it to detect frequency of micro-trap on atom chip is presented. The enhancement of scattering spectrum is due to a coherent Raman conversion between two different cavity modes mediated by collective vibrations of atoms through nonlinear opto-mechanical couplings. The physical conditions of this technique are roughly estimated on Rubidium atoms, and a simple quantum analysis as well as a multi-body semiclassical simulation on this nonlinear Raman process is conducted.

PACS numbers: 42.50.Nn; 37.30.+i; 37.10.Vz; 42.65.Dr;

I. INTRODUCTION

Similar to the technology of integrated circuits on electronic chips to control electrons, the micro-fabricated chips to manipulate cold atoms and molecules [1–3], ions and plasmas [4, 5] or massive nano-mechanical resonators [6] are now being actively pursued towards precise quantum measurements [7, 8] and information processing [9, 10]. Combined with different micro-fabricated elements [11], atom chips provide versatile integrated devices to precisely control particle's motion [12], biological cells [13], chemical reactions or material assembling [14–16] on a specially fabricated substrate to nanometer scales. Among these trends, controlling atomic motions in near-field potential plays an important role in coherent manipulation of atomic states. On atom chips, atoms can be confined above a surface where the electric, magnetic or optical fields [17] are built towards coherent manipulation on both internal and external degrees of freedom. The local forces produced on the chip can pack atoms into a micrometer-sized region ($< 1\mu m$) to a condition that the internal transitions and the external motions are intensely entangled [3, 8]. Indeed the motion of the atoms under a quantum confinement is always the main focus in all the above applications on atom chips.

Therefore, precise estimation of local potentials in which the atoms are confined becomes very crucial to identify the motion of the atoms in small scale. Considering modern optical trapping techniques [18], atoms can freely be controlled by highly focused near electromagnetic fields [19] on atom chips within microcavities and a real-time detection of local field along certain dimensions is an essential aspect to estimate the spatial distribution and the dynamic stability of confined atomic clouds under controls [20].

In order to estimate the trapping parameters of micro-traps, many different methods have been proposed, such as dynamical methods on atomic oscillations [21–23], the trap-loss rate method of atomic collisions [24], the free-expansion method by temperature measurement [25] and optical spectroscopic methods via stimulated Raman scattering (SRS) [26–28] or recoil induced resonance on atomic velocity [29–31]. Because the field-induced micro-trap on atom chips is relatively flexible on small scales, above mentioned mechanical methods on this system are difficult to carry out in a high resolution limit. The conventional optical probing methods are mainly based on stable absorptive spectrum related to incoherent radiation of atoms limited by the saturation effect [32] and the gain of the probe mode for a detection is weak [33]. Although SRS is a well-established technique on condensed materials, it has not been studied much in the context of atom-optics system [26, 31, 34].

In this paper, we demonstrate a high-gain pump-probe Raman spectrum on a trapped cold atomic ensemble [35] and propose a more convenient and sensitive method to diagnose micro-traps by using the coherent enhanced Raman spectrum in high finesse microcavity. Due to atomic recoil motion, atomic oscillations in the micro-trap will be actuated and closely entangled with resonant cavity modes through scattering in atomic absorption-emission cycles [29]. The dynamical backaction of the atomic oscillation dramatically modifies the optical spectrum and its intensity is further enhanced by a synchronization of the individual oscillators [36] (equivalent to building a collective mechanical mode). The fact that the optical spectrum of trapped atoms in high-finesse cavity is enhanced by cooperative vibrations [37] is the problem this paper seeks to address by developing a detection technique of microtrap on atom chips.

II. MODEL AND MECHANISM

The model under consideration concerns about a cold atomic gas of N identical atoms with transition frequency ω_0, mass m and trapped by an external potential approximately treated as an one-dimensional potential $V_{trap} = \frac{1}{2}m\nu_z^2 z^2$, which corresponds to a typical configuration on atom-chips [38, 39]. This is a reasonable assumption on cold atomic gas (e.g. BEC) for that the thermal atoms will concentrate more on lower vibration modes and the trap can be approximated by a harmonic potential. The trapped atomic gas is enclosed in a high-

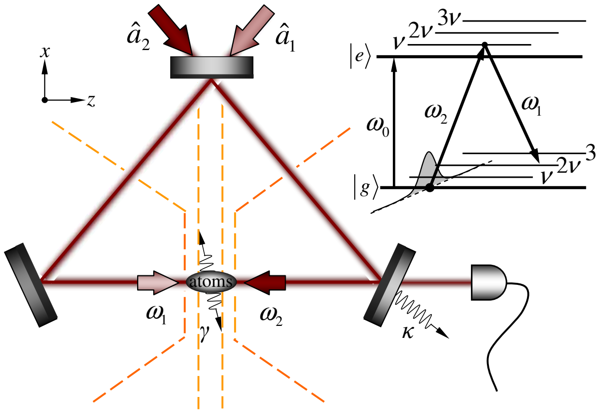

FIG. 1. The scheme of the probe-pump modes within a high-Q ring cavity. The dashed line is the circuit used to generate microtraps on the atom chip. The inset above right gives the level structure to demonstrate stimulated Raman transition, where the wave packet stands for initial thermal distribution and ν is the trapping frequency.

Q ring cavity towards employing a pump-probe scheme [41], in order to diagnose the trapping frequency ν_z that characterizes the effective trapping potential V_{trap}, by using two counter-propagating optical fields, a strong pump mode with frequency ω_2 to stimulate and a weak probe mode with frequency ω_1 to detect the atoms that are trapped in a near-field potential as shown in Fig.1. The direction of propagation for probe and pump modes are taken to be along $\pm z$ respectively, giving rise to the scheme of stimulated Raman scattering process. Our objective is to see the dependence of spectral gain of probe mode on trapping frequency ν_z that can be estimated by a measurable quantity, namely the detuning between pump and probe modes, $\delta_{21} = \omega_2 - \omega_1$ and analyze the mechanical environment of the atomic motion.

This kind of pump-probe scheme within a strong atom-cavity coupling regime in high-Q optical cavities is routinely considered in cavity QED experiments and within the reach of practical realizability now [37, 42, 45]. For our current purpose the high-Q cavity provides a low noise detection, which not only enhances atom-cavity coupling but also increases the sensitivity of measurement by a factor of $1/(1-R)$, where R is the reflectivity of cavity mirror [46]. Further, these requirements of the system enable a usage of Bonifacio's collective atomic recoil laser (CARL) model [47] to introduce an extra trapping potential [35] for the micro-trap on atom chip. Describing the two-level atomic gas with the Pauli spin operator $\hat{\sigma}^0$ and their internal transitions by $\hat{\sigma}^{\pm}$, pump and probe modes by $\hat{a}_2, \hat{a}_1$, the system Hamiltonian is [35],

$$
\begin{aligned}
\hat{H} = & \sum_{j=1}^{N}\left(\frac{\hat{p}_j^2}{2m} + \frac{1}{2}m\nu_z^2\hat{z}_j^2\right) + \hbar\omega_0\sum_{j=1}^{N}\hat{\sigma}_j^0 + \hbar\omega_1\hat{a}_1^\dagger\hat{a}_1 \\
& + \hbar\omega_2\hat{a}_2^\dagger\hat{a}_2 + i\hbar\left[g_1\hat{a}_1^\dagger\sum_{j=1}^{N}\hat{\sigma}_j^- e^{-ik_1\hat{z}_j} - H.c.\right] \\
& + i\hbar\left[g_2\hat{a}_2^\dagger\sum_{j=1}^{N}\hat{\sigma}_j^- e^{+ik_2\hat{z}_j} - H.c.\right], \qquad (1)
\end{aligned}
$$

where $g_1(g_2)$ is atom-probe(pump) coupling rate.

Before we embark upon estimating the potential, we shall now detail the mechanism of high-gain Raman scattering spectrum and how it can lead to estimating the trapping potential. The underlying mechanism of this model depends on a nonlinear effect due to a nonlinear coupling of atomic internal transitions with the vibration modes of the micro-trap. Identifying the position and momentum as

$$
\hat{z}_j = \sqrt{\frac{\hbar}{2m\nu_z}}(\hat{b}_j + \hat{b}_j^\dagger), \quad \hat{p}_j = -i\sqrt{\frac{\hbar m\nu_z}{2}}(\hat{b}_j - \hat{b}_j^\dagger),
$$

with $\hat{b}_j(\hat{b}_j^\dagger)$ being phonon annihilation(creation) operator of j^{th} atom and obeys bosonic commutation relation. Moving to the interaction picture with respect to the free part of Hamiltonian $\hat{H}_0 = \sum_{j=1}^{N}\hbar\nu_z\hat{b}_j^\dagger\hat{b}_j + \hbar\omega_0\sum_{j=1}^{N}\hat{\sigma}_j^0 + \hbar\omega_1\hat{a}_1^\dagger\hat{a}_1 + \hbar\omega_2\hat{a}_2^\dagger\hat{a}_2$, and using expanded Glauber displacement operator [48]

$$
\hat{D}(-i\eta) \equiv e^{-i\eta(\hat{b}_j^\dagger + \hat{b}_j)} = e^{-\eta^2/2}\sum_{n,m}\frac{(-i\eta)^{n+m}}{n!m!}\hat{b}_j^{\dagger n}\hat{b}_j^m,
$$

above Hamiltonian can be simplified to

$$
\begin{aligned}
\hat{H}_I = & i\hbar g_1 e^{-\eta_1^2/2}\sum_{j=1}^{N}\sum_{n,m}^{\infty}\frac{(-i\eta_1)^{n+m}}{n!m!}\hat{a}_1^\dagger\hat{b}_j^{\dagger n}\hat{b}_j^m\hat{\sigma}_j^- \\
& \times e^{i(\omega_1 + n\nu_z - m\nu_z - \omega_0)t} - H.c \\
& + i\hbar g_2 e^{-\eta_2^2/2}\sum_{j=1}^{N}\sum_{n,m}^{\infty}\frac{(i\eta_2)^{n+m}}{n!m!}\hat{a}_2^\dagger\hat{b}_j^{\dagger n}\hat{b}_j^m\hat{\sigma}_j^- \\
& \times e^{i(\omega_2 + n\nu_z - m\nu_z - \omega_0)t} - H.c. \qquad (2)
\end{aligned}
$$

Here the Lamb-Dicke parameter $\eta_i = k_i\sqrt{\hbar/2m\nu_z} \equiv \sqrt{\omega_{ri}/\nu_z}$ $(i = 1, 2)$ will further scale the opto-mechanical coupling with $\omega_{ri} = \hbar k_i^2/2m$ being the single-photon recoil frequency. This interaction Hamiltonian makes it easier to see the stimulated scattering initiated by cavity modes. Further the scattering amplitudes oscillate at an effective frequencies as indicated in the exponentials and depend on $\omega_{1,2}$. Since these frequencies can be arbitrarily controlled, one can immediately establish a resonance condition such that the time-dependence in the above

Hamiltonian can be coherently suppressed. Therefore we get,

$$\omega_1 - \omega_0 + (n-m)\,\nu_z = 0, \omega_2 - \omega_0 + (n'-m')\,\nu_z = 0,$$

which precisely leads to a resonant condition

$$\delta_{21} = (n' - m' + m - n)\nu_z = l\nu_z, \quad l = 0, \pm 1, \pm 2, \cdots, \tag{3}$$

where the integers l are the resonant scattering orders that can be used to label the gain peaks. We call this relation Raman resonant condition because the relation comes from Raman transitions between different cavity modes mediated by vibration modes of the trap $(\hat{b})$ and the gain shares a similar mechanism with Raman spectroscopy. When this condition is satisfied there occurs a maxima in the output spectrum, introduced in next section, and can be readily measured in a real experiment.

In addition, assuming $k_1 \approx k_2 = k$ leading to $\eta_1 \approx \eta_2 = \eta$ and $g_1 \approx g_2 = g$ for simplicity, which we do for numerical simulations, in resonant condition the Hamiltonian can be further simplified to

$$\hat{H}_I = i\hbar g e^{-\eta^2/2}\Bigg[\hat{a}_1^\dagger \sum_{j=1}^{N} \hat{\sigma}_j^- \sum_{n,m}^{\infty} \frac{(-i\eta)^{n+m}}{n!m!} \hat{b}_j^{\dagger n} \hat{b}_j^m + \hat{a}_2^\dagger \sum_{j=1}^{N} \hat{\sigma}_j^- \sum_{n,m}^{\infty} \frac{(i\eta)^{n+m}}{n!m!} \hat{b}_j^{\dagger n} \hat{b}_j^m\Bigg] - H.c.. \tag{4}$$

In the high-Q cavity with a strong atom-photon coupling strength [42], above Hamiltonian demonstrates an intense entanglement of the vibration mode $\hat{b}_j$ with internal transition $\hat{\sigma}_j^\pm$ through a nonlinear mechanical coupling coefficients η^n. If $\eta \ll 1$, only lower vibration modes are involved and the Hamiltonian can be expanded by a power series of η where the high-order Raman transitions are significantly depressed. In this case Eq.(4) will be simplified and a further analysis on the intensity of the peaks due to coherent transitions between lower vibration modes is possible within this N-body system and only the atoms distributed on lower vibration modes are critical in determining the gain of the corresponding Raman peak. However, height estimation of the peak l in the Raman spectrum becomes difficult when the Lamb-Dicke parameter $\eta \sim 1$ leading to a photon recoil frequency comparable to trap frequency ν_z and Raman transitions between higher vibration levels should be included. Nevertheless the simplified Hamiltonian in Eq.(4) gives an insight into the Raman process occurring due to coherent atomic motion.

A specific case which can highlight the elusive opto-mechanical coupling between the cavity mode and the atomic vibration is under the conditions of far off-resonant with low atomic saturation when the upper atomic levels can be adiabatically eliminated. Neglecting the weak probe and treating all the atoms in a homogenous pumping field, the far-off intense pumping mode induces an effective atomic polarization [43]

$$\hat{\sigma}_j^- \approx \frac{g}{i\delta_{20} - \gamma}\hat{a}_2,$$

which leads to a Hamiltonian

$$\hat{H}_I \approx \hbar\left(U_0 - i\Gamma_0\right)\hat{a}_2^\dagger \hat{a}_2 \sum_{j=1}^{N} e^{i\eta(\hat{b}_j^\dagger + \hat{b}_j)} + H.c., \tag{5}$$

where $\delta_{20} = \omega_2 - \omega_0$ is the detuning of the atom from the pumping field and γ is the atomic spontaneous emission rate. The above Hamiltonian clearly describes an opto-mechanical interaction that is extensively studied on cold atoms. Eq.(5) demonstrates that an opto-mechanical model for cold atoms are actually related to coherent motion of N atoms which is evaluated by the collective order parameter $R = \sum_{j=1}^{N} e^{ik\hat{z}_j}$. With large-detuned condition of $\delta_{20} \gg \gamma$, the light-shift coefficient U_0 and the incoherent scattering rate Γ_0 reduce to

$$U_0 = \frac{g^2\delta_{20}}{\delta_{20}^2 + \gamma^2} \approx \frac{g^2}{\delta_{20}}, \tag{6a}$$

$$\Gamma_0 = \frac{g^2\gamma}{\delta_{20}^2 + \gamma^2} \approx 0, \tag{6b}$$

respectively. Therefore an effective Hamiltonian under large-detuned pumping field reads

$$\hat{H}_I \approx \hbar\frac{2g^2}{\delta_{20}}\hat{a}_2^\dagger \hat{a}_2 \sum_{j=1}^{N} \cos\left(k\hat{z}_j\right),$$

with an effective opto-mechanical coupling clearly depending on the collective vibration modes of the N atoms. If all the atoms are synchronized on a same vibration mode, an extreme linear coupling rate is obtained by

$$G = \frac{2g^2 N}{\delta_{20}}, \tag{7}$$

whose strength can be greatly enhanced by the population numbers, N, on the vibration mode. Since the above interaction Hamiltonian is not limited with only the linear in $\hat{z}_j$, one can in general employ the methods in this work for high-order nonlinear displacements (Quadratic in position, for example [44]) of a mechanical oscillator due to radiation pressure of pumping mode proportional to intensity $\hat{a}_2^\dagger \hat{a}_2$.

III. GAIN SPECTRUM AND DETECTION

We now proceed with a further analysis by numerically simulations on the dynamical behavior of this multiple-body system on a general basis. The evolution of the density matrix $\hat{\rho}$ with cavity damping $\kappa_1(\kappa_2)$ and atomic spontaneous emission rate γ can be described with a master equation

$$\frac{d\hat{\rho}}{dt} = \frac{1}{i\hbar}[\hat{H}, \hat{\rho}] + \hat{\mathcal{L}}_j\hat{\rho} + \hat{\mathcal{L}}_f\hat{\rho}, \tag{8}$$

where the Louivillians

$$\hat{\mathcal{L}}_j\hat{\rho} = \frac{\gamma}{2}\sum_{j=1}^{N}\left(2\hat{\sigma}_j^-\hat{\rho}\hat{\sigma}_j^+ - \hat{\sigma}_j^+\hat{\sigma}_j^-\hat{\rho} - \hat{\rho}\hat{\sigma}_j^+\hat{\sigma}_j^-\right),$$

$$\hat{\mathcal{L}}_f\hat{\rho} = \frac{1}{2}\sum_{i=1,2}\kappa_i\left(2\hat{a}_i\hat{\rho}\hat{a}_i^\dagger - \hat{a}_i^\dagger\hat{a}_i\hat{\rho} - \hat{\rho}\hat{a}_i^\dagger\hat{a}_i\right),$$

and the semiclassical behavior can be investigated by the dynamic motion of expectation values $\langle\dot{O}\rangle = Tr(\dot{\hat{\rho}}\hat{O})$. We use the full Hamiltonian Eq. (1) so as to include higher order transitions as explained towards the end of previous section. Thus the equations of motion for relevant observables are,

$$\frac{d\theta_j}{d\tau} = p_j, \tag{9a}$$

$$\frac{dp_j}{d\tau} = -\nu^2\theta_j - A_1^*\sigma_j e^{-i\theta_j} - A_1\sigma_j^* e^{i\theta_j} + A_2(\sigma_j + \sigma_j^*), \tag{9b}$$

$$\frac{d\sigma_{zj}}{d\tau} = 2\rho\left[\left(A_1^* e^{-i\theta_j} + A_2\right)\sigma_j + \sigma_j^*\left(A_1 e^{i\theta_j} + A_2\right)\right] - \Gamma\left(\sigma_{0j} - 1\right) \tag{9c}$$

$$\frac{d\sigma_j}{d\tau} = i\left(\Delta_{20} + \frac{p_j}{2}\right)\sigma_j - \rho\sigma_{0j}\left(A_1 e^{i\theta_j} + A_2\right) - \Gamma\sigma_j, \tag{9d}$$

$$\frac{dA_1}{d\tau} = i\Delta_{21}A_1 + \frac{1}{N}\sum_{j=1}^{N}\sigma_j e^{-i\theta_j} - \kappa A_1, \tag{9e}$$

where the pump mode A_2 is in a strong coherent state and excluded from Eq.(9), sustaining by a stabilized locking driven field [45]. The dimensionless variables introduced in above equations are $\theta_j = 2k\langle\hat{z}_j\rangle$, $p_j = \frac{\langle\hat{p}_j\rangle}{\hbar k\rho}$, $\sigma_j = \left\langle\hat{\sigma}_j^- e^{ik_2\hat{z}_j}\right\rangle e^{i\omega_2 t}$, $\sigma_{0j} = -2\left\langle\hat{\sigma}_j^0\right\rangle$, $A_1 = \frac{\langle\hat{a}_1\rangle}{\sqrt{N\rho}}e^{i\omega_2 t}$, $\Delta_{21} = (\omega_2 - \omega_1)/(\omega_r\rho)$, $\Delta_{20} = (\omega_2 - \omega_0)/(\omega_r\rho)$, $\nu = \nu_z/(\omega_r\rho)$, $\Gamma = \gamma/(\omega_r\rho)$, $\kappa = \kappa_1/(\omega_r\rho)$ and $\tau = \omega_r\rho t$ assuming $k_1 \approx k_2 = k$ and $g_1 \approx g_2 = g$, for simplicity. The scaling parameters ω_r and ρ are photon recoil frequency $\omega_r = (2\hbar k)^2/2m$ and collective coupling constant $\rho = (g\sqrt{N}/\omega_r)^{2/3}$ respectively [47]. Among the above rescaled parameters, Δ_{20}, the frequency detuning of pump mode from the atomic transition, and Δ_{21}, the detuning between the pump mode and the probe mode, can be modulated in the experiment by frequency chirping method. The figure of merit, as in conventional CARL theory [47], is the time dependent gain function of the probe field A_1 and is given as

$$G\left(\Delta_{21}, \tau\right) = \frac{\left|A_1(\tau)\right|^2 - \left|A_1(0)\right|^2}{\left|A_1(0)\right|^2}, \tag{10}$$

where $A_1(0)$ is the initial amplitude of probe mode.

For our simulation, we use Rubidium atoms and the Lamb-Dicke parameter $\eta = \sqrt{\omega_r/\nu} \approx 0.4$ with maximum resonant number excited in Eq.(3) is about $l \approx \pm 15$ as shown in Fig.2. Therefore the contributions of the high-order Raman transitions will not be omitted beyond the Lamb-Dicke approximation and the use of original Hamiltonian Eq. (1) in equations of motion for observables Eq. (9) is needed. It is worth noting that, if the density of the atomic gas is increased in a stronger trap, the Lamb-Dicke parameter η will be small enough that the Raman transition will be closely concentrated around the central region of lower scattering numbers.

Our calculations on this system as shown in Fig.2 demonstrates a high gain of the weak probe mode [35, 49], and reveals a cavity enhanced Raman spectrum with a regular pectinate profile. The high-gain peaks of the spectrum are closely related to the collective atomic motion in the trap with a gain magnitude enhanced by population occupations of the atoms on different vibration modes [50]. Due to atomic recoil, the thermal atoms with an initial Gaussian velocity distribution (which is randomly distributed to N atoms at the initial time, see inset of Fig.1) are quickly redistributed to different oscillation modes through optical scattering supported by the high-Q cavity. Then the probe mode is amplified gradually by coherent Raman transitions between different vibration modes of the atoms and will be further improved by a synchronization of collective motion (see Eq.(7)). After the depletion of thermal atoms, line width of the gain peak is reduced by an elimination of Doppler broadening (see Fig.2) [51] and replaced by a comb like profile. Although this gain enhancement of the atoms in the trap has been observed in many experiments [33, 37, 52, 53], the Raman spectrum and the detection technique under this scheme is not purposely explored. In the present case, the enhanced gain of the probe mode detected at different times after a continuous-wave pumping turned on can be obtained by a frequency scanning process with chirping probe laser(see Ref.[45]). Fig.2(a) is the scanning spectrum of the probe mode obtained under the condition that the pump is red-detuned from the atomic transition frequency, while Fig.2(b) is in a resonant case and Fig.2(c) is blue detuned.

Although all the detunings in Fig.2 gives high resolution spectra with sharp peaks, the gain magnitude of the probe mode are actually in a different order after a same pumping time, τ. For resonant pumping, the maximum height of the peak at time $\tau = 20$ is about 10^2, which is almost one order smaller than that in the off-detuned spectrum (the gain magnitudes of the highest peaks are labeled in Fig.2). This difference is because that an off-detuned pumping will increase the absorption-emission recycling frequency to an effective Rabi frequency $\Omega_R \approx \sqrt{\Delta_{20}^2 + (2\rho A_2)^2 + \Gamma^2}$ and improve the saturation magnitude of atomic dispersion, indicating an optimal spectrum for dispersive atomic medium (see Eq.(6)) to establish coherent vibration modes. The off-detuned pumping also can suppress the spontaneous emission which introduces random motions into the coherent atomic oscillation in the trap and, thus, diminishes the spectral magnitude with a lower resolution. The other difference of these spectra is that the Raman transition shifts more into Stokes region by the red-detuned

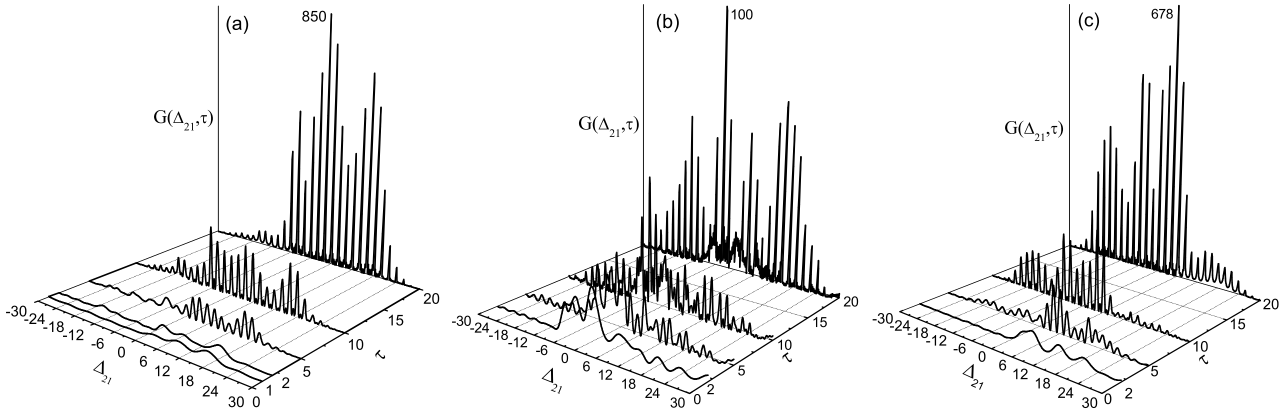

FIG. 2. The simulation of gain spectrum of the probe mode at different pumping time τ in a harmonic trap with the trapping frequency $\nu = 2$. (a) Red-detuned driving with $\Delta_{20} = -15$; (b) Resonant case with $\Delta_{20} = 0$; (c) Blue-detuned driving with $\Delta_{20} = 15$. The other parameters are $\rho = 3$, $A = 2$, $\Gamma = 1$, $\kappa = 0.01$. The number of the atoms in the trap is only $N = 100$. All the parameters are scaled by the collective recoil frequency $\rho\omega_r$.

driving (Fig2(a)) and shifts more into anti-Stokes region under the blue-detuned pumping (Fig2(c)). This is clearly due to the cooling and the heating effects of the red-detuned and the blue-detuned driving on atomic vibration modes, respectively.

The comb-like structure under all of the three pumping conditions implies a robust detection method of trapping potentials. By analyzing the frequency difference between two resonant peaks with a spectrometer, the intensity of a micro-trap along the pump-probe direction can be easily obtained. Fig.2 demonstrates that the minimum unit distance between two neighboring peaks of the gain spectrum is 2, which is exactly the trapping frequency ν along pumping direction. Clearly, the positions of the peaks in Fig.2 indicate a resonant condition of the pump-probe detuning of

$$\Delta_{21} = l\nu, \quad l = 0, \pm1, \pm2, \cdots, \tag{11}$$

and which definitely verifies quantum analysis Eq. (3).

Fig.2 also reveals that the gain of a probe mode is a time developing spectrum after the pumping mode is switched on, increasing with time first and, finally, stabilized by the saturation of synchronization and the damping process of the probe field and the atoms. Our simulations verify further that the response times to establish a high gain spectrum are very quick for all of the three pumping conditions. Without considering the isotope fraction and hyperfine structure, a rough response time of this spectrum on Rubidium atoms can be estimated. If the density of Rubidium gas loaded in the micro-trap is about 10^2 atoms/cm^3 ($\rho = 3$) and the atoms are driven by a strong field on $5^2P_{3/2} \longleftrightarrow 5^2S_{1/2}$ transition with $\lambda = 780nm$, then the collective recoil frequency $\rho\omega_r$ of the gas is about 2.88×10^5 Hz, and the time interval needed to develop a detectable high-gain spectrum is about 69.4 microseconds ($\tau = 20$), and which is a reasonable time in a typical experiment. If the density of the atom is increased to 10^8 atoms/cm^3 in a stronger micro-trap, the building time for a high-gain spectrum will be only 1.0 microseconds. Increasing the atom-field coupling g in the high-Q cavity will also speed up the synchronization process of collective motion and shorten the response time of the spectrum. Compared with other detection methods [23, 24], this proposal provides a quicker and precise measurement on potential parameters for a micro-trap if the system is connected to a computer assisted spectroanalysis with a chirping probe fields at an optimal ramping rate [45].

When the response time of the gain reduces below one nanosecond, a pulse wave pump-probe detection might be employed on a highly dense atomic gas in a strong trap [54]. Surely this pump-probe Raman scattering method can also be used to analyze other types of traps (e.g., anharmonic traps) as long as the collective motion of the atoms can be coherently stimulated by an electric, magnetic or optical force during the mode scanning process of the detection.

IV. CONCLUSION

In order to identify the mechanical stiffness of the local micro-trap on atom chips, an opto-mechanical measurement on the frequency of the trap based on a high-gain Raman scattering spectrum of probe mode in a ring cavity has been proposed. This Raman scattering spectrum owns a distinct pectinate profile with high resonant peaks, narrow spectral lines and develops with the pumping time. The spectral gain is derived from a resonant Raman scattering of pumping mode to probe mode on atomic vibration motion and enhanced by synchronized collective motion of atoms (corresponding to coherent vibration mode) established in the trap. The narrowed peak width comes from a removal of the Doppler broadening through a coherent distribution of initial thermal atoms into different vibration modes in the trap. This Raman pump-probe spectroscopy for depth measurement of micro-traps is quick and more sensitive than that of the traditional methods, and can be further developed into a rapid detecting method on surface vibration dynamics or on surface plasmon oscillations. Because trapping and guiding ions, atoms, molecules or even plasma with nanofabricated circuits on atom chips are all closely related to collective motions, the method we presented here is universal to detect different micro-traps as long as the coherent motion can be efficiently coupled with internal atomic transition by the nonlinear Raman scattering process. A concise quantum analysis of this high-gain Raman spectrum reveals a nonlinear opto-mechanical coupling of atomic vibration with two cavity modes mediated by atomic internal level transitions. This nonlinear gain mechanism also provides an insight into the stimulated Raman spectrum of vibrating atoms on condensed materials or gives a clue on the enhanced Raman spectrum of bound electrons on a structured metal surface.

Certainly, the distinct profile of the Raman scattering spectrum of probe mode in this paper depends on how well one can satisfy the approximations we adopted in this work. The first approximation is an assumption of a one-dimensional harmonic potential for cold trapped atomic gases. A more general trapping potential on atom chips, often taking a 3-D periodic arrangement, will lead to a more complicated spectral structure with nonuniform peaks and more broadened lines or even optical band. Nevertheless the proposed method can still provide useful information about the intensity of the trapping potentials along a certain direction because of its opto-mechanical mechanism. The second approximation is related to the two-level assumption of the N trapped identical atoms which omits also the isotope fraction [32, 41] and the hyperfine level structure [55, 56] which could lead to different Raman resonant relations of Eq.(3) and results in an overlap of different groups of Raman peaks. Finally, the spectral line broadening mechanisms by atomic collision, random spontaneous emission, beam collimation or by source linewidth [41] are all neglected in the calculation of the Raman scattering gain spectrum.

ACKNOWLEDGEMENT

This work was supported by the Shaanxi Provincial Natural Science Foundation SJ08A12, PRC.

[1] R. Folman, P. Krüger, J. Schmiedmayer, J. Denschlag, C. Henkel, Adv. At. Mol. Opt. Phys. **48**, 263 (2002).
[2] S. A. Meek, H. Conrad and G. Meijer, Science **324** 1699 (2009).
[3] Y. Colombe, T. Steinmetz, G. Dubois, F. Linke, D. Hunger and J. Reichel, Nature **450** 272 (2007).
[4] D. Stick, W. K. Hensinger, S. Olmschenk, M. J. Madsen, K. Schwab and C. Monroe, Nature Physics **2** 36 (2006).
[5] Shanhui Fan, Nature photonics **4** 76 (2010).
[6] G. Anetsberger, R. Rivière, A. Schliesser, O. Arcizet and T. J. Kippenberg, Nature Photonics **2** 627 (2008).
[7] A. Cronin, Nature Phys. **2**, 661 (2006).
[8] M. F. Riedel, P. Böhi, Y. Li, T. W. Hänsch, A. Sinatra and P. Treutlein, Nature **464**, 1170 (2010).
[9] R. Dumke, M. Volk, T. Müther, F. B. J. Buchkremer, G. Birkl, and W. Ertmer, Phys. Rev, Lett. **89**, 097903 (2002).
[10] G. Birkl and J. Fortágh, Laser Photon. Rev. **1**, 12 (2007).
[11] M Wallquist, K Hammerer, P Rabl, M Lukin and P Zoller, Phys. Scr. T **137** 014001 (2009).
[12] R. Folman, P. Krüger, D. Cassettari, B. Hessmo, T. Maier, and J. Schmiedmayer, Phys. Rev, Lett. **84**, 4749 (2000).
[13] P. Y. Chiou, A. T. Ohta and M. C. Wu, Nature **436** 370 (2005).
[14] M. Bonn, A.W. Kleyn, G.J. Kroes, Surf. Sci. **500**, 475 (2002).
[15] A. J. deMello, Nature **442** 394 (2006).
[16] P. Jensen, Rev. Mod. Phys. **71**, 1695 (1999).
[17] J. Reichel, V. Vuletić, *Atom Chips* (WILEY-VCH Verlag GmbH and Co. KGaA, Weinheim, 2011).
[18] S. Erikkson, Eur. Phys. J. D **35**, 135 (2005).
[19] M. Hammes, D. Rychtarik, H.-C. Nägerl, and R. Grimm, Phys. Rev. A **66**, 051401(R) (2002).
[20] T. Walker, D. Sesko and C. Wieman, Phys. Rev. Lett. **64**, 408 (1990).
[21] K. Kim, K. H. Lee, M. Heo, H. R. Noh and W. Jhe, Phys. Rev. A **71**, 053406 (2005).
[22] K. Kim, H. R. Noh and W. Jhe, Phys. Rev. A **71**, 033413 (2005).
[23] G. Moon, M. S. Heo, Y. Kim, H. R. Noh and W. Jhe, Phys. Rev. A **81**, 033425 (2010).
[24] D. Hoffmann, S. Bali, and T. Walker, Phys. Rev. A **54**, R1030 (1996).
[25] C. D. Wallace, T. P. Dinneen, K. Y. N. Tan, A. Kumarakrishnan, P. L. Gould and J. Javanainen, J. Opt. Soc. Am. B **11**, 703 (1994).
[26] D. Grison, B. Lounis, C. Salomon, J. Y. Courtois and G. Grynberg, Europhys. Lett. **15**, 149 (1991).
[27] T. M. Brzozowski, M. Brzozowska, J. Zachorowski, M. Zawada and W. Gawlik, Phys. Rev. A **71**, 013401 (2005).
[28] Y. Yoshikawa, Y. Torii, and T. Kuga, Phys. Rev. Lett. **94**, 083602 (2005).
[29] D. R. Meacher, D. Boiron, H. Metcalf, C. Salomon, and G. Grynberg, Phys. Rev. A **50**, R1992 (1994).
[30] M. Kozuma, Y. Imai, K. Nakagawa, and M. Ohtsu, Phys. Rev. A **52**, R3421 (1995).
[31] M. Brzozowska, T. M. Brzozowski, J. Zachorowski, and W. Gawlik, Phys. Rev. A **73**, 063414 (2006).
[32] K. Razdan and D. A. Van Baak, Am. J. Phys. **67**, 832 (1999).
[33] D. Kruse, Ch. von Cube, C. Zimmermann, and Ph. W. Courteille, Phys. Rev. Lett. **91**, 183601 (2003).

[34] B. Lounis, P. Verkerk, J.-Y. Courtois, C. Salomon and G. Grynberg, Europhys. Lett. **21**, 13 (1993).

[35] G. J. Yang, L. Zhang, and W. Shu, Phys. Rev. A **68**, 063802 (2003).

[36] C. von Cube, S. Slama, D. Kruse, C. Zimmermann, Ph. W. Courteille, G. R. M. Robb, N. Piovella and R. Bonifacio, Phys. Rev. Lett. **93**, 083601 (2004).

[37] B. Nagorny, Th. Elsässer and A. Hemmerich, Phys. Rev. Lett. **91**, 153003 (2003).

[38] P. Horak, B.G. Klappauf, A. Haase, R. Folman, J. Schmiedmayer, P. Domokos and E. A. Hinds, Phys. Rev. A **67**, 043806 (2003).

[39] P. Quinto-Su, M. Tscherneck, M. Holmes, and N. Bigelow, Opt. Express **12**, 5098 (2004).

[40] P. Horak, K. M. Gheri and H. Ritsch, Phys. Rev. A **52**, 554 (1995).

[41] M. Himsworth and T. Freegarde, Phys. Rev. A **81**, 023423 (2010).

[42] J. McKeever, A. Boca, A. D. Boozer, J. R. Buck and H. J. Kimble, Nature **425**, 268 (2003).

[43] P. Domokos and H. Ritsch, J. Opt. Soc. Am. B **20** 1098 (2003).

[44] C. A. Holmes and G. J. Milburn, Fortschr. Phys. **57** 1052 (2009).

[45] D. Kruse, M. Ruder, J. Benhelm, C. von Cube, C. Zimmermann, Ph W. Courteille, T. Elsässer, B. Nagorny and A. Hemmerich, Phys. Rev. A **67**, 051802(R) (2003).

[46] S. Ezekiel, Sov. J. Quantum Electron. **8**, 942 (1978).

[47] R. Bonifacio, L. De Salvo, L. M. Narducci, E. J. D'Angelo, Phys. Rev. A **50**, 1716 (1994).

[48] W. Vogel and R. L. de Matos Filho, Phys. Rev. A **52**, 4214 (1995).

[49] L. Zhang, G. Y. Yang and L. X. Xia, J. Opt. B: Quantum Semiclass. Opt. **7**, 355 (2005).

[50] P. S. Jessen, C. Gerz, P. D. Lett, W. D. Phillips, S. L. Rolston, R. J. C. Spreeuw and C. I. Westbrook, Phys. Rev. Lett. **69**, 49 (1992).

[51] V. S. Letokhov and B. D. Pavlik, Appl. Phys. **9**, 229 (1976).

[52] S. Slama, S. Bux, G. Krenz, C. Zimmermann and Ph W. Courteille, Phys. Rev. Lett. **98**, 053603 (2007).

[53] J. Ringot, P. Szriftgiser and J. C. Garreau, Phys. Rev. A **65**, 013403 (2001).

[54] D. Polli, D. Brida, S. Mukamel, G. Lanzani, and G. Cerullo, Phys. Rev. A **82**, 053809 (2010).

[55] D. A. Smith and I. G. Hughes, Am. J. Phys. **72**, 631 (2004).

[56] T. Zigdon, A. D. Wilson-Gordon, and H. Friedmann, Phys. Rev. A **77**, 033836 (2008).